Differential Antiviral Response of Endothelial Cells after Infection with Pathogenic and Nonpathogenic Hantaviruses

Annette A. Kraus,[1,2] Martin J. Raftery,[1] Thomas Giese,[3] Rainer Ulrich,[1] Rainer Zawatzky,[4]
Stefan Hippenstiel,[2] Norbert Suttorp,[2] Detlev H. Krüger,[1] and Günther Schönrich[1]*

*Institut für Virologie[1] and Klinik für Innere Medizin m.S. Infektiologie,[2] Charité-Universitätsmedizin Berlin,
D-10098 Berlin, and Institut für Immunologie, Universität Heidelberg,[3] and Forschungsschwerpunkt
Angewandte Tumorvirologie, Deutsches Krebsforschungszentrum,[4] D-69120 Heidelberg, Germany*

Hantaviruses represent important human pathogens and can induce hemorrhagic fever with renal syndrome (HFRS), which is characterized by endothelial dysfunction. Both pathogenic and nonpathogenic hantaviruses replicate without causing any apparent cytopathic effect, suggesting that immunopathological mechanisms play an important role in pathogenesis. We compared the antiviral responses triggered by Hantaan virus (HTNV), a pathogenic hantavirus associated with HFRS, and Tula virus (TULV), a rather nonpathogenic hantavirus, in human umbilical vein endothelial cells (HUVECs). Both HTNV- and TULV-infected cells showed increased levels of molecules involved in antigen presentation. However, TULV-infected HUVECs upregulated HLA class I molecules more rapidly. Interestingly, HTNV clearly induced the production of beta interferon (IFN-β), whereas expression of this cytokine was barely detectable in the supernatant or in extracts from TULV-infected HUVECs. Nevertheless, the upregulation of HLA class I on both TULV- and HTNV-infected cells could be blocked by neutralizing anti-IFN-β antibodies. Most strikingly, the antiviral MxA protein, which interferes with hantavirus replication, was already induced 16 h after infection with TULV. In contrast, HTNV-infected HUVECs showed no expression of MxA until 48 h postinfection. In accordance with the kinetics of MxA expression, TULV replicated only inefficiently in HUVECs, whereas HTNV-infected cells produced high titers of virus particles that decreased after 48 h postinfection. Both hantavirus species, however, could replicate equally well in Vero E6 cells, which lack an IFN-induced MxA response. Thus, delayed induction of antiviral MxA in endothelial cells after infection with HTNV could allow viral dissemination and contribute to the pathogenesis leading to HFRS.

The rodent-borne hantaviruses belong to a family of enveloped negative-sense RNA viruses, the *Bunyaviridae*, and represent an emerging threat to human health (28, 35). These spherical particles of 80 to 110 nm contain a single-stranded tripartite RNA genome of negative polarity encoding four proteins: the RNA-dependent RNA polymerase, the nucleocapsid (N) protein, and two envelope glycoproteins, G1 and G2 (16). Transmission can occur when humans inhale aerosols of excreta derived from chronically infected rodents. In general, different hantaviruses show different degrees of virulence in humans. Tula virus (TULV) is a hantavirus species that is considered nonpathogenic to humans (46), although it may cause symptoms in rare cases (18, 36). On the other hand, pathogenic hantavirus species can cause severe disease: hantavirus cardiopulmonary syndrome (HCPS) and hemorrhagic fever with renal syndrome (HFRS) (20). The most severe cases of HFRS are due to infection with Hantaan virus (HTNV), which occurs in Asia (21).

Prominent features of clinical hantavirus infections include fever, thrombocytopenia, and capillary leakage. However, the underlying mechanisms are still obscure. It is well documented that hantaviruses replicate in endothelial cells without causing a direct cytopathic effect (31, 43, 49). This suggests that the

hantavirus-induced immune response itself plays a pivotal role in the cascade of events leading to endothelial dysfunction (32). Several findings support this concept. For example, certain HLA alleles elevate the risk for a severe clinical course of hantavirus infection (24, 25). Recently, HTNV has been shown to infect and thereby activate human dendritic cells, which represent the most efficient stimulators of T lymphocytes (33). In line with this finding, increased numbers of stimulated CD8+ T cells have been observed in blood from patients with acute severe hantavirus-associated disease (1, 14, 29). Surprisingly, high frequencies of memory CD8+ T lymphocytes can be found a long time after the clinical hantavirus infection has resolved (45). Moreover, CD8+ T cells have been detected in association with hantavirus-infected lung endothelial cells by immunohistochemical analysis of specimens derived from HCPS patients (29, 49). In kidney biopsy specimens of patients with HFRS, infiltrating CD8+ cells have been localized near the tubuli (42). Finally, hantavirus-infected endothelial cells have been shown to secrete chemokines that attract T lymphocytes (40).

The antiviral response of virus-infected cells is mediated principally by alpha/beta interferon (IFN-α/β) (37). IFN-α/β is not only synthesized in response to virus infection but is also produced at low levels in the absence of virus infection (41). These cytokines upregulate the expression of antigen-presenting molecules such as HLA class I, which are recognized by cytotoxic CD8+ T cells, thus eliminating virus-infected cells. In addition, IFN-α/β stimulates a network of genes encoding fac-

---

* Corresponding author. Mailing address: Institut für Virologie, Charité-Universitätsmedizin Berlin, Schumannstrasse 20/21, D-10117 Berlin, Germany. Phone: 49-30-450-525071. Fax: 49-30-450-525907. E-mail: guenther.schoenrich@charite.de.

tors with direct antiviral activity. Among these, the MxA protein has been shown to inhibit the growth of hantaviruses (6, 17). It has been demonstrated that the MxA protein intracellularly sequesters the viral N protein of La Crosse virus, another member of the *Bunyaviridae*, in cytoplasmic inclusions (19). Such a mechanism could interfere with the production of new viral particles, because the N protein is an essential viral component. Thus, upregulation of HLA class I molecules and induction of the MxA protein are important antiviral parameters that could control viral growth and determine the outcome of infections with different hantaviruses.

In the present study we compared the capacities of these pathogenic and nonpathogenic hantaviruses to induce an antiviral response in endothelial cells. For this purpose, we comparatively analyzed the growth of HTNV and TULV in human umbilical vein endothelial cells (HUVECs) and Vero E6 cells. Moreover, we investigated the expression of antigen presentation molecules and the production of IFN-α/β in HTNV- and TULV-infected cells. Finally, we explored the induction of the MxA protein by HTNV and TULV in HUVECs.

MATERIALS AND METHODS

Cells. HUVECs were prepared by the method of Jaffe et al. (15) as modified by Thornton et al. (44). Cultures of HUVECs were grown on gelatin-coated plates. Confluent cells in the second passage were used for experiments. HUVECs were maintained in MCDB131 (Gibco BRL, Karlsruhe, Germany) supplemented with 10% fetal calf serum, 100 IU of penicillin/ml, 100 μg of streptomycin/ml, 1 μg of amphotericin B/ml, 4.5 mM L-glutamine, and 20 μg of endothelial-cell growth factor/ml. Vero E6 cells and A549 cells (48) were maintained in Dulbecco's modified Eagle's medium supplemented with 10% fetal calf serum, 100 IU of penicillin, 100 μg of streptomycin/ml, and 4.5 mM L-glutamine. The medium and fetal calf serum were certified endotoxin free by the manufacturers.

Viruses. Stocks of HTNV (strain 76-118) and TULV (strain Moravia) were propagated on Vero E6 cells. Supernatant was collected from cell cultures at day 14 postinfection, cleared of cell debris by centrifugation at 2,000 × g, aliquoted, and frozen at −80°C. Concentrated viral stocks were prepared by pelleting virus from supernatants of infected cells at 130,000 × g for 2 h at 4°C. Virus pellets were resuspended in Tris-HCl buffer (pH 7.6) and stored at −80°C until use. Virus stocks were free of mycoplasma as tested by PCR. For infection, equal quantities of viable virus or UV-inactivated HTNV (mock infection) were allowed to adsorb to HUVECs for 1 h at 37°C. UV irradiation for 5 min completely inactivated HTNV, corresponding to a reduction of at least 6 log scales in the viral titer. The titer of viable virus in the supernatant of hantavirus-infected cells was determined by infection of Vero E6 cells and counting of foci in a chemiluminescence detection assay (13). Stocks of encephalomyocarditis virus (EMCV) were generated as described previously (48).

Flow cytometry and immunocytochemistry. For surface immunofluorescence analysis by flow cytometry, cells in suspension were washed once with an ice-cold washing solution (phosphate-buffered saline [PBS] with 1% heat-inactivated fetal calf serum and 0.05% sodium azide) before being resuspended with the first antibody in ice-cold blocking solution (PBS with 10% heat-inactivated fetal calf serum and 0.2% sodium azide) for 1 h. Cells were then washed twice in ice-cold washing solution, and staining was repeated with a fluorescein isothiocyanate (FITC)-coupled goat anti-mouse secondary antibody. After the final staining step, cells were washed twice in ice-cold washing solution and resuspended in 2 ml of PBS with 1% formaldehyde. Tubes were left at 4°C overnight before being centrifuged. The cells were resuspended in 200 μl of PBS with 0.2% formaldehyde before being measured. Flow cytometry was performed using a FACScalibur (Becton Dickinson, Heidelberg, Germany).

For immunocytochemistry, infected cells were transferred to slides, incubated overnight at 37°C, and then fixed with acetone-methanol (1:1) at 4°C for 30 min. Slides were washed three times in PBS and incubated for 1 h at room temperature with the first antibody in blocking solution (PBS with 10% heat-inactivated species-specific serum). Cells were then washed again three times in PBS and subsequently stained with the secondary antibodies in blocking solution. Finally, cells were washed and embedded in mounting medium, and slides were stored at 4°C before being analyzed.

The following antibodies were used for flow cytometry and immunocytochemistry: anti-ICAM-1 (clone HA58), purchased from PharMingen, Heidelberg, Germany, and anti-HLA I (clone W6/32), obtained from Serotec, Oxford, United Kingdom. For detection of HTNV in immunocytochemistry analysis, monoclonal antibody 1C12, specific for the hantavirus nucleocapsid protein (22, 23), or an HTNV-cross-reactive human serum derived from a hantavirus (Dobrava)-infected patient was used. Expression of TULV antigen was determined by incubating cells with a rabbit serum raised against the *Escherichia coli*-expressed N protein of TULV strain Malacky (39). As secondary antibodies, an FITC-coupled goat anti-mouse serum and an FITC-coupled swine anti-rabbit serum (DAKO, Hamburg, Germany) were employed.

Quantification of IFN. Concentrations of IFN-α and IFN-β in supernatants harvested from infected cells were quantified by using a sandwich enzyme-linked immunosorbent assay (ELISA) kit (R&D Systems, Wiesbaden, Germany) according to the manufacturer's instructions.

In addition, a bioassay was conducted for quantification of IFN activity (48). For this purpose, supernatants from infected HUVECs were transferred to A549 indicator cells (3 × 10^4/well). On the next day, the cells were infected with EMCV. After 26 to 30 h, the medium was removed. To quantify the cytopathic effect, cells were fixed with 4% glutaraldehyde and stained with 1% crystal violet. The dye was solubilized in 33% acetic acid, and the optical density of the eluate was measured at 570 nm in a Labsystem Multiscan MS ELISA reader. The amount of IFN is expressed in international reference units per milliliter, by use of exogenously added National Institutes of Health human IFN as a reference. Poly(I·C) obtained from Sigma (Munich, Germany) was used to stimulate production of IFN-α/β in control cells.

Detection of MxA protein. The expression of MxA protein was analyzed by Western blotting. Cell extracts were prepared by lysing cells in lysis buffer containing 10 mM Tris-HCl (pH 7.4), 1 mM EDTA, 100 mM NaCl, 1 mM phenylmethylsulfonyl fluoride, 1% Triton X-100 (wt/vol), and protease inhibitors (10 μg/ml). Cell lysates were subjected to sodium dodecyl sulfate-polyacrylamide gel electrophoresis (SDS-PAGE) on a 10% gel with 50 μg of protein per lane. Following electrophoretic separation, the proteins were electrotransferred to Immobilon-P transfer membranes (Millipore, Schwalbach, Germany) in blotting buffer (25 mM Tris, 192 mM glycine, 20% methanol). Thereafter, blots were blocked for 1 h at room temperature in high-salt Tris-buffered saline, consisting of 50 mM Tris-HCl (pH 8.0), 500 mM NaCl, 0.05% (wt/vol) Tween 20, and 5% (wt/vol) skim milk. Blots were incubated overnight at 4°C with a murine anti-β-actin antibody (ab 6276; Abcam Ltd., Cambridge, United Kingdom) or the mouse anti-MxA monoclonal antibody M143 (5). The blots were then washed three times with high-salt Tris-buffered saline, followed by incubation with peroxidase-conjugated rabbit anti-mouse immunoglobulin G (Amersham Pharmacia Biotech, Dreieich, Germany) for 1 h at room temperature. After final washing steps, the blots were developed by ECL (Amersham Pharmacia Biotech).

RNA sample preparation. Cells (10^6) were lysed with 300 μl of MagnaPure lysis buffer (Roche Applied Science, Mannheim, Germany), and samples were frozen at −80°C. After thawing, lysates were mixed and transferred to Magna-Pure sample cartridges, and mRNA was isolated with a MagnaPure-LC device by using a standard protocol. The elution volume was set to 50 μl. One aliquot (8.2 μl) of RNA was reverse transcribed in a thermocycler by using avian myeloblastosis virus reverse transcriptase (RT) and oligo(dT) as the primer (first-strand cDNA synthesis kit for RT-PCR; Roche Applied Science) according to the manufacturer's protocol. After termination of cDNA synthesis, the reaction mixture was diluted to a final volume of 500 μl and stored at −20°C until PCR analysis.

LightCycler PCR. Target sequences were amplified by using LightCycler primer sets (Search-LC, Heidelberg, Germany) with the LightCycler FastStart DNA Sybr Green I kit (Roche Diagnostics) according to the manufacturer's protocol. RNA input was normalized by the average expression of the housekeeping genes encoding β-actin and cyclophilin B. Copy numbers were calculated from a virtual standard curve, obtained by plotting a known input concentration of a plasmid against the PCR cycle number at which the detected fluorescence intensity reached a fixed value. Data from two independent analyses for each sample and parameter were averaged and presented as adjusted transcripts per microliter of cDNA or as ratios to control values.

Statistical methods and formula. A paired Student's *t* test was used to analyze intergroup differences (see Fig. 2 and 3). A *P* value of <0.05 was considered significant. The percentage of inhibition of HLA class I enhancement on HUVECs by anti-IFN-β antibodies (see Fig. 4) was calculated on the basis of the respective mean fluorescence intensity (MFI) as follows: percent inhibition = {[(MFI for HTNV-infected cells − MFI for uninfected cells) − (MFI for HTNV-infected cells with anti-IFN-β antibodies − MFI for uninfected cells)]/(MFI for HTNV-infected cells − MFI for uninfected cells)} ×100.
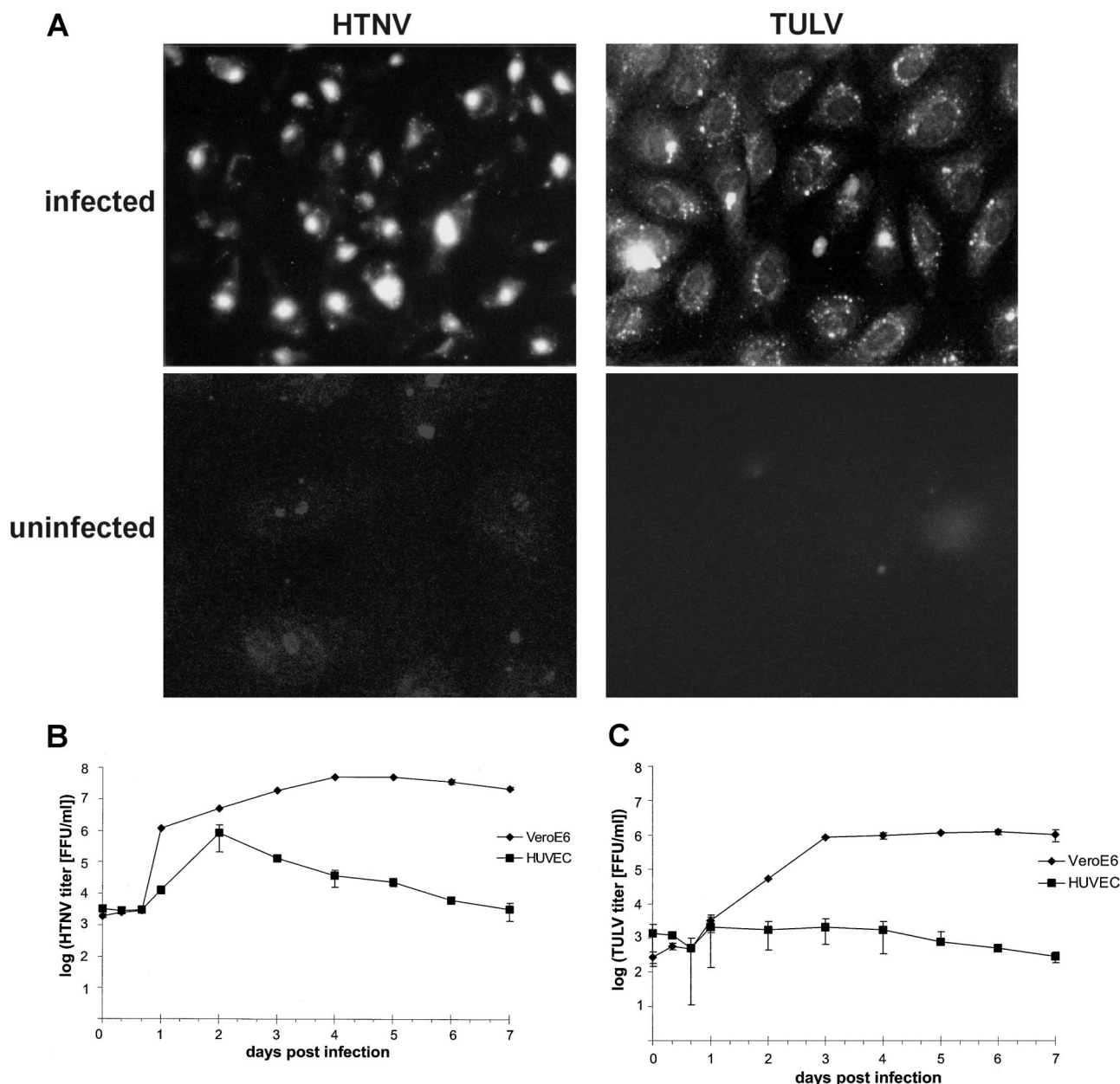
FIG. 1. Detection of viral antigen and kinetics of virus production in HTNV- and TULV-infected cells. HUVECs or Vero E6 cells were infected (MOI, 1) with HTNV or TULV. (A) At 3 days postinfection, the distribution of viral antigen was visualized by immunocytochemistry in TULV-infected HUVECs by using a rabbit-derived polyclonal antiserum and in HTNV-infected HUVECs by using monoclonal antibody 1C12, specific for the hantavirus N protein. In both cases approximately 80 to 85% of cells stained positive. As a negative control, uninfected HUVECs were included in the analyses. Magnification, ×63. (B and C) Kinetics of virus production by HTNV-infected (B) and TULV-infected (C) HUVECs and Vero E6 cells are shown on a log scale. Supernatants of infected cells were collected at the time points indicated, and virus titers were determined by a chemiluminescence detection assay (13). Results are means ± standard errors of the means from three individual experiments with cells from three different donors (HUVECs) or from two individual experiments (Vero E6 cells).

RESULTS

HTNV and TULV replicate in endothelial cells with different efficiencies. Infection of endothelial cells is a hallmark of hantavirus-associated pathogenesis. Therefore, we investigated whether both HTNV and TULV could grow efficiently in endothelial cells. For this purpose we infected HUVECs (at a multiplicity of infection [MOI] of 1) with HTNV or TULV and

then analyzed the expression of viral proteins by immunocytochemistry (Fig. 1A). At day 3 after infection with HTNV or TULV, we could detect viral proteins in 80 to 85% of HUVECs, whereas no viral antigen expression was found in uninfected control cells. In the next step, we measured the kinetics of virus production by HTNV-infected (Fig. 1B) or TULV-infected (Fig. 1C) HUVECs or Vero E6 cells. By use of

a chemiluminescence assay (13) we observed that cells infected with TULV produced much fewer viral particles than HTNV-infected HUVECs. For example, at day 2 postinfection, the viral titer produced by HTNV-infected cells was 10^6 focus-forming units (FFU)/ml, whereas in the supernatants of TULV-infected HUVECs, only 10^3 FFU/ml were detected. Figure 1B demonstrates that until day 2 postinfection, HTNV could replicate in HUVECs nearly as efficiently as in Vero E6 cells lacking IFN-α/β genes (3). Thereafter, viral titers produced by HTNV-infected HUVECs declined whereas viral titers produced by HTNV-infected Vero E6 cells remained high. In contrast, TULV-infected HUVECs produced only low viral titers, showing no peak, compared to titers in TULV-infected Vero E6 cells (Fig. 1C). These results indicate that both HTNV and TULV can successfully enter HUVECs, resulting in expression of viral proteins. Both hantavirus species can grow efficiently in Vero E6 cells lacking IFN-α/β genes. In HUVECs, however, HTNV, but not TULV, creates a time window from 16 to 48 h postinfection in which it can efficiently replicate and disseminate.

HTNV and TULV modulate antigen presentation molecules on endothelial cells with different kinetics. We then investigated the consequences of hantavirus infection for expression of molecules that are required for recognition by antiviral T lymphocytes. For this purpose we infected HUVECs (MOI = 1) with HTNV or TULV and measured the density of HLA class I molecules by flow cytometry at different time points postinfection. Both HTNV- and TULV-infected cells showed strongly augmented expression of HLA class I molecules at day 3 postinfection (Fig. 2A). Kinetic analyses revealed that TULV-infected HUVECs upregulated HLA class I molecules more rapidly, with a peak at days 2 to 3 postinfection (Fig. 2B). In contrast, HTNV-infected HUVECs increased expression of HLA class I molecules more gradually, reaching peak levels at days 4 to 5 postinfection. These phenotypic changes were not observed after mock infection of HUVECs with UV-inactivated HTNV or after infection with a low virus dose (MOI = 0.1) (data not shown). We also analyzed the expression of HLA class II molecules on HUVECs after infection with hantaviruses. Neither HTNV- nor TULV-infected HUVECs expressed HLA class II molecules, whereas HUVECs treated with IFN-γ stained strongly positive (data not shown). Taken together, these results show that both HTNV and TULV drastically enhance the endothelial expression of HLA class I molecules, albeit with different kinetics.

HTNV and TULV induce different levels of IFN-α/β in endothelial cells. In the next series of experiments, we investigated the upregulation of HLA class I molecules in further detail. Most viruses induce the production of IFN-α/β, which can enhance the expression of HLA class I molecules (37). For this reason we investigated the synthesis of IFN-α/β by HTNV- and TULV-infected HUVECs. As a positive control we used HUVECs treated with poly(I · C), a synthetic "mimic" of double-stranded viral RNA. Figure 3A shows that HUVECs treated with poly(I · C) for 24 h released large amounts of IFN-β, whereas infected cells produced much less of the cytokine as determined by ELISA. In supernatants from HTNV-infected HUVECs we always found larger amounts of IFN-β than in supernatants collected from cultures of TULV-infected HUVECs. Neither HTNV nor TULV induced HUVECs to
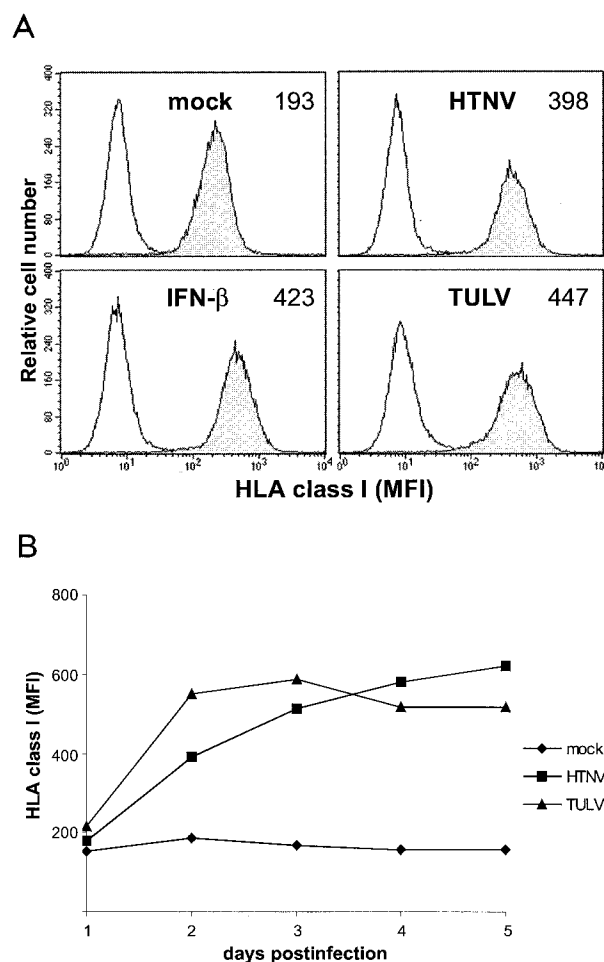
FIG. 2. Temporal pattern of HLA class I expression on HTNV- and TULV-infected HUVECs. HUVECs were infected (MOI = 1) with HTNV, TULV, or UV-inactivated HTNV (mock infection). (A) Histograms show HLA class I expression at day 3 postinfection as indicated. As a positive control, HUVECs were treated with IFN-β (20,000 U/ml for 24 h). Shaded curves, expression of HLA class I; open curves, staining of cells with an irrelevant antibody (isotype control). On the x axis, the fluorescence intensity (log scale, 4 decades) is shown, whereas the y axis depicts the relative cell number. The MFI is given in the upper right corner of each histogram. Results shown are representative of eight separate experiments with cells derived from eight different donors. (B) The kinetics of HLA class I expression on HTNV- and TULV-infected HUVECs were analyzed. The y axis shows the MFI at days 0 to 5 postinfection as indicated. Results of one representative experiment out of eight are shown.

secrete IFN-α (data not shown). This result prompted us to investigate IFN production by employing a bioassay that measures antiviral activity in the supernatants of infected cells. Again, in supernatants from poly(I · C)-treated control cells or HTNV-infected cells, we could detect antiviral activity, whereas antiviral activity was barely detectable in supernatants from TULV-infected HUVECs (data not shown). We also monitored the production of IFN-α/β on the mRNA level. For this purpose we used real-time quantitative RT-PCR (Fig. 3B). This type of analysis revealed that HTNV increases the production of IFN-β mRNA after infection starting at day 2, reaching peak levels at day 4, and decreasing thereafter. In
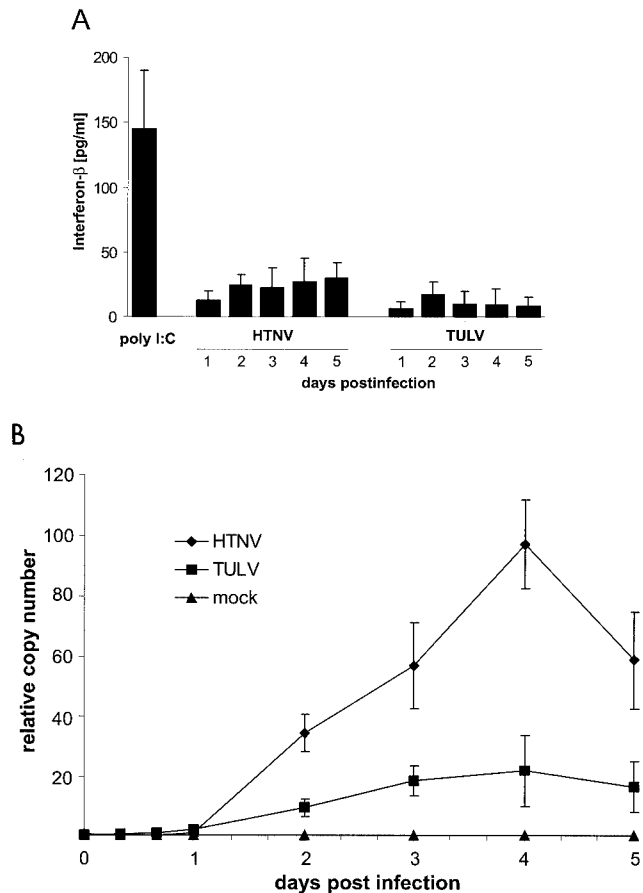
A

B

FIG. 3. Production of IFN-β by endothelial cells after infection with HTNV or TULV. (A) An ELISA technique was used to analyze supernatants from infected (MOI = 1) HUVECs collected at the time points indicated. As a positive control, supernatants from cells treated with poly(I · C) (10 μg/ml for 24 h) were included. Concentrations (in picograms per milliliter) are given as means ± standard errors of the means from three individual experiments with cells derived from three different donors. (B) Quantitative real-time RT-PCR analysis was performed to determine the relative copy numbers of IFN-β transcripts in infected (MOI = 1) HUVECs. As a control, cells were infected (MOI = 1) with UV-inactivated HTNV (mock infection). Results are means ± standard errors of the means from three individual experiments with cells from three different donors.

comparison, TULV-infected HUVECs produced only small amounts of IFN-β transcripts, whereas mock infection (with UV-inactivated HTNV) had no effect. Neither HTNV- nor TULV-infected HUVECs showed induction of IFN-α, IFN-γ, or IFN-λ gene transcription (data not shown). Taken together, these findings suggest that HTNV elicits a stronger IFN-β response than TULV, most likely due to more efficient replication.

IFN-β mediates upregulation of HLA class I molecules on HTNV- and TULV-infected endothelial cells. We then analyzed the contribution of IFN-β to the observed modulation of HLA class I molecules on HTNV- and TULV-infected HUVECs. For this purpose we employed neutralizing anti-IFN-β antibodies (Fig. 4). In cultures of HTNV-infected HUVECs, the presence of neutralizing anti-IFN-β antibodies strongly reduced (78% inhibition) upregulation of HLA class I

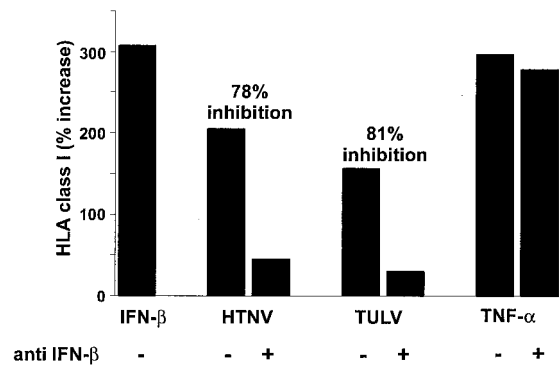
FIG. 4. Inhibition of HLA class I upregulation on HTNV- and TULV-infected endothelial cells by anti-IFN-β antibodies. HUVECs were either infected (MOI = 1) or left uninfected. As a positive control, cells were stimulated with TNF-α (10 ng/ml for 24 h) or IFN-β (20,000 U/ml for 24 h). Some cells were treated simultaneously with anti-IFN-β antibodies (2,000 U/ml). Expression levels of HLA class I molecules were determined by fluorescence-activated cell sorter analysis at day 3 postinfection. The percentage of increase in MFI over that for uninfected control cells is given on the y axis. In addition, the percentage of inhibition of HLA class I enhancement by anti-IFN-β antibodies was calculated (see Materials and Methods) and is shown above the respective columns.

molecules. In contrast, neutralizing anti-IFN-α antibodies had no effect (data not shown). In addition, we tested whether neutralizing anti-IFN-β antibodies could interfere with TULV-induced HLA class I upregulation. Despite the fact that TULV induced comparatively small amounts of IFN-β, HLA class I enhancement could be efficiently blocked by anti-IFN-β antibodies (81% inhibition). In contrast, anti-IFN-β antibodies did not prevent the upregulation of HLA class I molecules on uninfected control cells that had been treated with tumor necrosis factor alpha (TNF-α). In conclusion, these experiments indicate that IFN-β is for the most part responsible for the HTNV- and TULV-induced increase of HLA class I molecules on HUVECs.

HTNV- and TULV-infected endothelial cells show different kinetics of MxA protein expression. Besides upregulation of molecules involved in antigen presentation, IFN-α and -β also induce the production of factors that play a crucial role in the innate immune response against viruses. Among these, the MxA protein can interfere with the replication of members of the *Bunyaviridae*. Because pathogenic and nonpathogenic hantaviruses replicate with different efficiencies in endothelial cells, we wanted to analyze whether HTNV and TULV differentially regulate the induction of MxA protein in HUVECs. To this end we determined the kinetics of MxA protein expression by performing Western blot analysis with extracts from infected HUVECs (Fig. 5). In comparison to HUVECs treated with poly(I · C) (positive control), HTNV-infected HUVECs showed a slow onset of MxA expression (48 h after infection). In contrast, in TULV-infected HUVECs, the MxA protein was already detectable at 16 h postinfection. These results indicate that HTNV and TULV induce MxA with different kinetics, which could explain the reduced replication rate of TULV in endothelial cells.
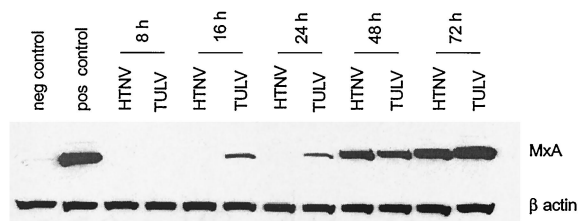
FIG. 5. Kinetics of MxA protein expression in HUVECs infected with HTNV or TULV. Cells were infected (MOI = 1), and lysates were prepared at different time points as indicated and analyzed by Western blotting. Lysates of cells incubated for 72 h in the absence of virus were used as a negative control, whereas lysates of cells stimulated with poly(I·C) (10 µg/ml for 24 h) served as a positive control. Expression of β-actin was determined as a control for the proper loading of SDS-PAGE gels. Results shown are representative of three independent experiments with cells derived from three different donors.

DISCUSSION

In humans, pathogenic hantaviruses cause endothelial dysfunction. However, the underlying mechanisms are poorly understood. We compared the antiviral responses elicited by a pathogenic (HTNV) and a nonpathogenic (TULV) hantavirus in endothelial cells in order to define potentially important immunopathological events. Both HTNV and TULV infection enhanced the expression of HLA class I molecules, albeit with different kinetics. HNTV induced higher levels of IFN-β than TULV. Most strikingly, the kinetics of MxA expression were different: TULV-infected cells showed an early onset of MxA expression (16 h postinfection), whereas HTNV-induced MxA appeared relatively late (48 h postinfection). Accordingly, viral titers produced by TULV-infected HUVECs were much lower than those produced by HTNV-infected HUVECs, which generated peak titers at 48 h postinfection. In contrast, Vero E6 cells, lacking IFN-α/β genes (3), supported efficient growth of both HTNV and TULV. Our results suggest that HTNV, but not TULV, can delay the IFN-β-induced antiviral MxA response and allow efficient viral replication during a time window of 48 h postinfection.

The expression of HLA class I molecules is essential for the adaptive and innate antiviral immune response. These molecules serve as recognition elements for T cells and regulate natural killer (NK) cell function (26). We observed a drastic increase in the density of HLA class I molecules after infection with either HTNV or TULV. In line with these results, another study found increased levels of HLA class I mRNA in hantavirus-infected HUVECs (10). The induction of HLA class I expression was not observed after infection at an MOI of 0.1 despite the high sensitivity of the cytofluorimetric analysis compared to ELISA-based methods (data not shown). This may explain negative data from a previous study (40). Neither HTNV nor TULV augmented the expression of HLA class II molecules on HUVECs as revealed by cytofluorimetric analyses (data not shown).

Many viruses enhance the expression of HLA class I molecules indirectly through induction of IFN-α/β (34, 37). In the supernatants of HTNV-infected HUVECs we could detect moderate levels of IFN-β. In comparison, less IFN-β was found in the supernatants of TULV-infected cells. Neither

HTNV-infected nor TULV-infected cells released IFN-α (data not shown). Given the fact that induction of IFN-α/β by viruses is primarily controlled at the transcriptional level, we also employed quantitative real-time PCR for more detailed analysis. We found peak levels of IFN-β mRNA in probes derived from HTNV-infected HUVECs at day 4 postinfection. Similarly, in human endothelial cells from saphenous veins, increased IFN-β mRNA levels were found at day 3 but not at day 1 after infection with HTNV (31). In addition, HTNV-induced IFN-β mRNA production was also observed by Geimonen et al. in DNA array analyses at day 4 postinfection (10). The levels of IFN-β mRNA in TULV-infected HUVECs were much lower than those in HTNV-infected cells. Moreover, no induction of IFN-α, IFN-γ, or IFN-λ was found by quantitative real-time RT-PCR (data not shown). In accordance with these findings, it has been reported recently that Prospect Hill virus, another nonpathogenic hantavirus, fails to induce significant IFN-β mRNA levels in HUVECs (10). The comparatively low levels of IFN-β mRNA in endothelial cells infected with nonpathogenic hantaviruses could be due to inefficient viral replication and hence to low production of double-stranded RNA, which triggers the synthesis of IFN-α/β.

The similar kinetics of HTNV-induced IFN-β production and HLA class I expression suggested that this cytokine was responsible for the observed HLA class I upregulation. Indeed, by using neutralizing antibodies, we could show that IFN-β is crucial for this phenotype. Anti-IFN-β but not anti-IFN-α antibodies could block up to 78% of the virus-induced effect. Important human pathogens from several other RNA virus families also induce HLA class I expression through IFN-β on various cell types. It is known that human parainfluenza virus type 3 and respiratory syncytial virus increase the levels of HLA class I molecules on respiratory epithelial cells via IFN-β production (8, 9). Similarly, IFN-β mediates induction of HLA class I expression on a glioma cell line and on HUVECs after infection with measles virus (2). Moreover, the HLA class I expression induced by West Nile virus could be abolished to a large extent by antibodies directed against IFN-α/β (38). Unexpectedly, HLA class I enhancement associated with TULV-infection could also be prevented (up to 81%) with neutralizing anti-IFN-β antibodies, although TULV-infected cells produced only small amounts of IFN-β. It has been demonstrated that a weak IFN-β signal induced by autocrine/paracrine cytokine secretion is an essential component in a positive feedback loop (41) that could trigger a shortcut in the activation of the antiviral defense. In fact, induction of interferon-stimulated genes without enhanced synthesis of IFN-α/β has been described for virus-infected cells (27) and could involve cellular receptors that recognize viral pathogen-associated molecular patterns (4). Thus, pathogenic hantaviruses such as HTNV might be able to interfere with a weak IFN-β signal, thereby disrupting the positive feedback loop and preventing an early antiviral MxA response.

The MxA proteins are IFN-induced GTPases that play a crucial role in the antiviral response against certain negative-strand RNA viruses (11, 47): *Orthomyxoviridae* (influenza A virus [30] and Thogoto virus [7]), *Rhabdoviridae* (vesicular stomatitis virus [30]), and *Bunyaviridae* (La Crosse virus [6], Rift Valley fever virus [6], sandfly fever virus [6], and HTNV [6, 17]). It has been shown that MxA interferes with the transport

of the viral N protein to the Golgi compartment, where assembly of hantaviruses takes place (12). Through this mechanism the N protein is no longer available for the assembly of new virus particles, and viral titers drop. By using Western blot analysis, we could detect induction of MxA expression in HUVECs as early as 16 h after infection with TULV. This suggests that TULV allows weak IFN-β signaling that is involved in rapid induction of MxA expression. In this way TULV replication could be blocked at an early time point, resulting in low virus titers. However, on Vero E6 cells, which are known to lack IFN-α/β genes and fail to mount an antiviral MxA response (3), TULV could grow as efficiently as HTNV. Supporting this view, in transfected Vero E6 cells expressing MxA, the replication of TULV is abolished (17). In contrast, HTNV delayed the MxA response in endothelial cells until 48 h postinfection. By this means the pathogenic hantavirus species creates a time window from 16 to 48 h postinfection in which it can replicate nearly as efficiently as in Vero E6 cells. We observed that the peak titer was reached concomitantly with the appearance of MxA and subsequently declined. Taken together, these data suggest that pathogenic but not nonpathogenic hantaviruses are able to block the early antiviral immune response in human endothelial cells.

HLA class I molecules, which serve as target structures for antiviral T cells, could be relevant for hantavirus-associated pathogenesis, as the severity of the clinical course in humans may correlate with HLA type (24, 25). In addition it has been observed previously that HTNV can infect and activate dendritic cells, which efficiently stimulate T lymphocytes (33). It is conceivable that a delayed MxA response could allow pathogenic hantaviruses to spread more efficiently in the endothelial cell layer and upregulate HLA class I molecules on a higher proportion of cells. Accordingly, antiviral CD8+ T lymphocytes may cause more damage during elimination of cells infected with HTNV. In addition, increased IFN-β release by endothelial cells infected with pathogenic hantaviruses could aggravate inflammatory processes that possibly contribute to endothelial dysfunction. Although the precise functional consequences of these differences between pathogenic and nonpathogenic hantaviruses remain to be elucidated in vivo, they are most likely important for the pathogenesis of hantavirus-associated diseases.

REFERENCES

1. **Chen, L. B., and W. S. Yang.** 1990. Abnormalities of T cell immunoregulation in hemorrhagic fever with renal syndrome. J. Infect. Dis. **161:**1016–1019.
2. **Dhib-Jalbut, S. S., and E. P. Cowan.** 1993. Direct evidence that interferon-

beta mediates enhanced HLA-class I expression in measles virus-infected cells. J. Immunol. **151:**6248–6258.
3. **Diaz, M. O., S. Ziemin, M. M. Le Beau, P. Pitha, S. D. Smith, R. R. Chilcote, and J. D. Rowley.** 1988. Homozygous deletion of the alpha- and beta 1-interferon genes in human leukemia and derived cell lines. Proc. Natl. Acad. Sci. USA **85:**5259–5263.
4. **Doyle, S., S. Vaidya, R. O'Connell, H. Dadgostar, P. Dempsey, T. Wu, G. Rao, R. Sun, M. Haberland, R. Modlin, and G. Cheng.** 2002. IRF3 mediates a TLR3/TLR4-specific antiviral gene program. Immunity **17:**251–263.
5. **Flohr, F., S. Schneider-Schaulies, O. Haller, and G. Kochs.** 1999. The central interactive region of human MxA GTPase is involved in GTPase activation and interaction with viral target structures. FEBS Lett. **463:**24–28.
6. **Frese, M., G. Kochs, H. Feldmann, C. Hertkorn, and O. Haller.** 1996. Inhibition of bunyaviruses, phleboviruses, and hantaviruses by human MxA protein. J. Virol. **70:**915–923.
7. **Frese, M., G. Kochs, U. Meier-Dieter, J. Siebler, and O. Haller.** 1995. Human MxA protein inhibits tick-borne Thogoto virus but not Dhori virus. J. Virol. **69:**3904–3909.
8. **Gao, J., B. P. De, and A. K. Banerjee.** 1999. Human parainfluenza virus type 3 up-regulates major histocompatibility complex class I and II expression on respiratory epithelial cells: involvement of a STAT1- and CIITA-independent pathway. J. Virol. **73:**1411–1418.
9. **Garofalo, R., F. Mei, R. Espejo, G. Ye, H. Haeberle, S. Baron, P. L. Ogra, and V. E. Reyes.** 1996. Respiratory syncytial virus infection of human respiratory epithelial cells up-regulates class I MHC expression through the induction of IFN-β and IL-1α. J. Immunol. **157:**2506–2513.
10. **Geimonen, E., S. Neff, T. Raymond, S. S. Kocer, I. N. Gavrilovskaya, and E. R. Mackow.** 2002. Pathogenic and nonpathogenic hantaviruses differentially regulate endothelial cell responses. Proc. Natl. Acad. Sci. USA **99:**13837–13842.
11. **Haller, O., M. Frese, and G. Kochs.** 1998. Mx proteins: mediators of innate resistance to RNA viruses. Rev. Sci. Tech. **17:**220–230.
12. **Haller, O., and G. Kochs.** 2003. Interferon-induced Mx proteins: dynamin-like GTPases with antiviral activity. Traffic **3:**710–717.
13. **Heider, H., B. Ziaja, C. Priemer, A. Lundkvist, J. Neyts, D. H. Krüger, and R. Ulrich.** 2001. A chemiluminescence detection method of hantaviral antigens in neutralisation assays and inhibitor studies. J. Virol. Methods **96:**17–23.
14. **Huang, C., B. Jin, M. Wang, E. Li, and C. Sun.** 1994. Hemorrhagic fever with renal syndrome: relationship between pathogenesis and cellular immunity. J. Infect. Dis. **169:**868–870.
15. **Jaffe, E. A., R. L. Nachman, C. G. Becker, and C. R. Minick.** 1973. Culture of human endothelial cells derived from umbilical veins. Identification by morphologic and immunologic criteria. J. Clin. Investig. **52:**2745–2756.
16. **Jonsson, C. B., and C. S. Schmaljohn.** 2001. Replication of hantaviruses. Curr. Top. Microbiol. Immunol. **256:**15–32.
17. **Kanerva, M., K. Melen, A. Vaheri, and I. Julkunen.** 1996. Inhibition of Puumala and Tula hantaviruses in Vero cells by MxA protein. Virology **224:**55–62.
18. **Klempa, B., H. Meisel, S. Räth, J. Bartel, R. Ulrich, and D. H. Krüger.** 2003. Occurrence of renal and pulmonary syndrome in a region of North-East Germany where Tula hantavirus circulates. J. Clin. Microbiol. **41:**4894–4897.
19. **Kochs, G., C. Janzen, H. Hohenberg, and O. Haller.** 2002. Antivirally active MxA protein sequesters La Crosse virus nucleocapsid protein into perinuclear complexes. Proc. Natl. Acad. Sci. USA **99:**3153–3158.
20. **Krüger, D. H., R. Ulrich, and A. Lundkvist.** 2001. Hantavirus infections and their prevention. Microbes Infect. **3:**1129–1144.
21. **Lee, H. W., and G. van der Groen.** 1989. Hemorrhagic fever with renal syndrome. Prog. Med. Virol. **36:**62–102.
22. **Lundkvist, A., A. Fatouros, and B. Niklasson.** 1991. Antigenic variation of European haemorrhagic fever with renal syndrome virus strains characterized using bank vole monoclonal antibodies. J. Gen. Virol. **72:**2097–2103.
23. **Lundkvist, A., H. Meisel, D. Koletzki, H. Lankinen, F. Cifire, A. Geldmacher, C. Sibold, P. Gott, A. Vaheri, D. H. Krüger, and R. Ulrich.** 2002. Mapping of B-cell epitopes in the nucleocapsid protein of Puumala hantavirus. Viral Immunol. **15:**177–192.
24. **Makela, S., J. Mustonen, I. Ala-Houhala, M. Hurme, J. Partanen, O. Vapalahti, A. Vaheri, and A. Pasternack.** 2002. Human leukocyte antigen-B8-DR3 is a more important risk factor for severe Puumala hantavirus infection than the tumor necrosis factor-alpha(-308) G/A polymorphism. J. Infect. Dis. **186:**843–846.
25. **Mustonen, J., J. Partanen, M. Kanerva, K. Pietila, O. Vapalahti, A. Pasternack, and A. Vaheri.** 1996. Genetic susceptibility to severe course of nephropathia epidemica caused by Puumala hantavirus. Kidney Int. **49:**217–221.
26. **Natarajan, K., N. Dimasi, J. Wang, R. A. Mariuzza, and D. H. Margulies.** 2002. Structure and function of natural killer cell receptors: multiple molecular solutions to self, nonself discrimination. Annu. Rev. Immunol. **20:**853–885.
27. **Navarro, L., K. Mowen, S. Rodems, B. Weaver, N. Reich, D. Spector, and M. David.** 1998. Cytomegalovirus activates interferon immediate-early response gene expression and an interferon regulatory factor 3-containing interferon-

stimulated response element-binding complex. Mol. Cell. Biol. **18:**3796–3802.

28. **Nichol, S. T.** 2001. Bunyaviruses, p. 1603–1633. *In* D. M. Knipe, P. M. Howley, D. E. Griffin, R. A. Lamb, M. A. Martin, B. Roizman, and S. E. Straus (ed.), Fields virology, 4th ed. Lippincott Williams & Wilkins, Philadelphia, Pa.

29. **Nolte, K. B., R. M. Feddersen, K. Foucar, S. R. Zaki, F. T. Koster, D. Madar, T. L. Merlin, P. J. McFeeley, E. T. Umland, and R. E. Zumwalt.** 1995. Hantavirus pulmonary syndrome in the United States: a pathological description of a disease caused by a new agent. Hum. Pathol. **26:**110–120.

30. **Pavlovic, J., T. Zurcher, O. Haller, and P. Staeheli.** 1990. Resistance to influenza virus and vesicular stomatitis virus conferred by expression of human MxA protein. J. Virol. **64:**3370–3375.

31. **Pensiero, M. N., J. B. Sharefkin, C. W. Dieffenbach, and J. Hay.** 1992. Hantaan virus infection of human endothelial cells. J. Virol. **66:**5929–5936.

32. **Peters, C. J., and S. R. Zaki.** 2002. Role of the endothelium in viral hemorrhagic fevers. Crit. Care Med. **30:**S268–S273.

33. **Raftery, M. J., A. Kraus, R. Ulrich, D. H. Krüger, and G. Schönrich.** 2002. Hantavirus infection of dendritic cells. J. Virol. **76:**10724–10733.

34. **Samuel, C. E.** 2001. Antiviral actions of interferons. Clin. Microbiol. Rev. **14:**778–809.

35. **Schmaljohn, C. S., and J. W. Hooper.** 2001. *Bunyaviridae*: the viruses and their replication, p. 1581–1602. *In* D. M. Knipe, P. M. Howley, D. E. Griffin, R. A. Lamb, M. A. Martin, B. Roizman, and S. E. Straus (ed.), Fields virology, 4th ed. Lippincott Williams & Wilkins, Philadelphia, Pa.

36. **Schultze, D., A. Lundkvist, U. Blauenstein, and P. Heyman.** 2002. Tula virus infection associated with fever and exanthema after a wild rodent bite. Eur. J. Clin. Microbiol. Infect. Dis. **21:**304–306.

37. **Sen, G. C.** 2002. Viruses and interferons. Annu. Rev. Microbiol. **55:**255–281.

38. **Shen, J., S. S. T-To, L. Schrieber, and N. J. King.** 1997. Early E-selectin, VCAM-1, ICAM-1, and late major histocompatibility complex antigen induction on human endothelial cells by flavivirus and comodulation of adhesion molecule expression by immune cytokines. J. Virol. **71:**9323–9332.

39. **Sibold, C., H. Meisel, D. H. Krüger, M. Labuda, J. Lysy, O. Kozuch, M. Pejcoch, A. Vaheri, and A. Plyusnin.** 1999. Recombination in Tula hantavirus evolution: analysis of genetic lineages from Slovakia. J. Virol. **73:**667–675.

40. **Sundstrom, J. B., L. K. McMullan, C. F. Spiropoulou, W. C. Hooper, A. A. Ansari, C. J. Peters, and P. E. Rollin.** 2001. Hantavirus infection induces the expression of RANTES and IP-10 without causing increased permeability in human lung microvascular endothelial cells. J. Virol. **75:**6070–6085.

41. **Taniguchi, T., and A. Takaoka.** 2002. A weak signal for strong responses: interferon-alpha/beta revisited. Nat. Rev. Mol. Cell. Biol. **2:**378–386.

42. **Temonen, M., J. Mustonen, H. Helin, A. Pasternack, A. Vaheri, and H. Holthofer.** 1996. Cytokines, adhesion molecules, and cellular infiltration in nephropathia epidemica kidneys: an immunohistochemical study. Clin. Immunol. Immunopathol. **78:**47–55.

43. **Temonen, M., O. Vapalahti, H. Holthofer, M. Brummer-Korvenkontio, A. Vaheri, and H. Lankinen.** 1993. Susceptibility of human cells to Puumala virus infection. J. Gen. Virol. **74:**515–518.

44. **Thornton, S. C., S. N. Mueller, and E. M. Levine.** 1983. Human endothelial cells: use of heparin in cloning and long-term serial cultivation. Science **222:**623–626.

45. **Van Epps, H. L., M. Terajima, J. Mustonen, T. P. Arstila, E. A. Corey, A. Vaheri, and F. A. Ennis.** 2002. Long-lived memory T lymphocyte responses after hantavirus infection. J. Exp. Med. **196:**579–588.

46. **Vapalahti, O., A. Lundkvist, S. K. Kukkonen, Y. Cheng, M. Gilljam, M. Kanerva, T. Manni, M. Pejcoch, J. Niemimaa, A. Kaikusalo, H. Henttonen, A. Vaheri, and A. Plyusnin.** 1996. Isolation and characterization of Tula virus, a distinct serotype in the genus *Hantavirus*, family *Bunyaviridae*. J. Gen. Virol. **77:**3063–3067.

47. **Weber, F., and R. M. Elliott.** 2002. Antigenic drift, antigenic shift and interferon antagonists: how bunyaviruses counteract the immune system. Virus Res. **88:**129–136.

48. **Yousefi, S., M. R. Escobar, and C. W. Gouldin.** 1985. A practical cytopathic effect/dye-uptake interferon assay for routine use in the clinical laboratory. Am. J. Clin. Pathol. **83:**735–740.

49. **Zaki, S. R., P. W. Greer, L. M. Coffield, C. S. Goldsmith, K. B. Nolte, K. Foucar, R. M. Feddersen, R. E. Zumwalt, G. L. Miller, and A. S. Khan.** 1995. Hantavirus pulmonary syndrome. Pathogenesis of an emerging infectious disease. Am. J. Pathol. **146:**552–579.